

Collective Dynamics at RHIC

A.H. Tang

Physics Department, P.O. Box 5000, Brookhaven National Laboratory, Upton,
NY 11973, aihong@bnl.gov

Abstract. The property of the “perfect liquid” created at RHIC is probed with anisotropic flow measurements. Different initial conditions and their consequences on flow measurements are discussed. The collectivity is shown to be achieved fast and early. The thermalization is investigated with the ratio of v_4/v_2^2 . Measurements from three sectors of soft physics (HBT, flow and strangeness) are shown to have a simple, linear, length scaling. Directed flow is found to be independent of system size.

1. Introduction: the perfect liquid

As the world’s first heavy ion collider, RHIC has initiated new opportunities for studying nuclear matter under extreme conditions. After six years of successful operations, the discovery of the existence of a perfect liquid in ultra-relativistic heavy ion collisions was announced[1]. Indications of liquid-like behavior of the matter that RHIC has created came in the form of large elliptic flow. Because of the pressure developed early in the collision, the initial spatial deformation due to geometry, which is quantified by eccentricity (ϵ), is converted into the asymmetry in the momentum space, which is quantified by elliptic flow (v_2)[2]. This conversion process is directly related to the thermalization, equation of state, etc. The wealth of data collected and analyzed in many aspects, including but not limited to elliptic flow, indicates that central Au+Au collisions can be well described by ideal Hydrodynamics[3]. It suggests that particles in the medium interact with one another rather strongly, which surprised many theoretists who had anticipated an almost ideal, weakly interacting gas. What is more interesting is that, this liquid has little viscosity and acts like a perfect one[4]. This is shown in Fig. 1, in which v_2 from data as a function of transverse momentum (p_T) is compared to the calculation with sound attenuation length (Γ_s) scaled by the time scale of the expansion τ_o . The sound attenuation length is related to the shear viscosity (η) by $\Gamma_s = \frac{4}{3}\eta(e+p)$, where e and p are energy density and pressure, respectively. We can see that as expected, viscosity reduces v_2 . The calculation shows that in order to explain the large v_2 observed at RHIC, one has to assume that the medium has an extremely small viscosity – the characteristic feature of a perfect liquid.

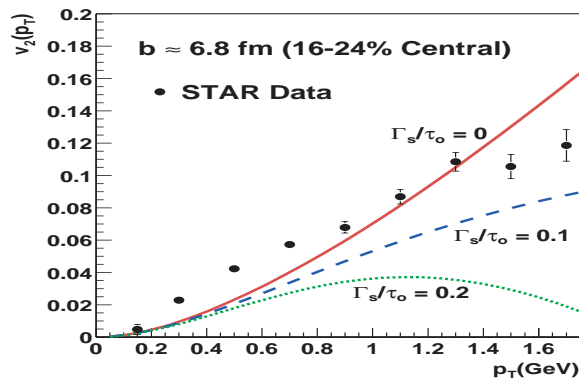


Figure 1. Elliptic flow v_2 as a function of p_T for different values of Γ_s/τ_o . The data points are four-particle cumulant data from the STAR Collaboration[5]. The difference between the ideal and viscous curves is linearly proportional to Γ_s/τ_o . This plot is from[4].

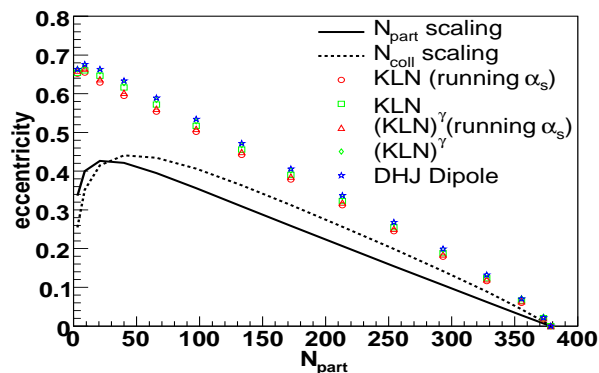


Figure 2. Initial spatial eccentricity ϵ at midrapidity as a function of the number participants for 200 GeV Au+Au collisions from various CGC models (see[7] for the detail description of CGC models). For comparison, the initial conditions where the initial parton density at midrapidity scales with the transverse density of wounded nucleons (full line) and of binary collisions (dotted line) are also shown. This plot is from[7]

2. The initial condition

The viscosity is so small that the initial spatial eccentricity is converted to momentum anisotropy with a high efficiency, and this process results in large amount of v_2 as reported by RHIC experiments. In this explanation one assumes that the initial spatial eccentricity is from Glauber source[6]. Recent theoretical work (Fig. 2) shows that a different initial condition like Color Glass Condensate (CGC) will give a much larger initial spatial eccentricity than that is from Glauber source. As a consequence of that, the viscosity has to be finite, as opposed to the close-to-zero viscosity in a perfect liquid, in order to reduce the v_2 to the level that matches the data. Thus the matter that RHIC has created can be explained either by a perfect liquid with a Glauber source or, a viscous matter with a CGC source. To distinguish between the two, one has to understand the initial condition. However it is not easy to trace the initial condition, because with it

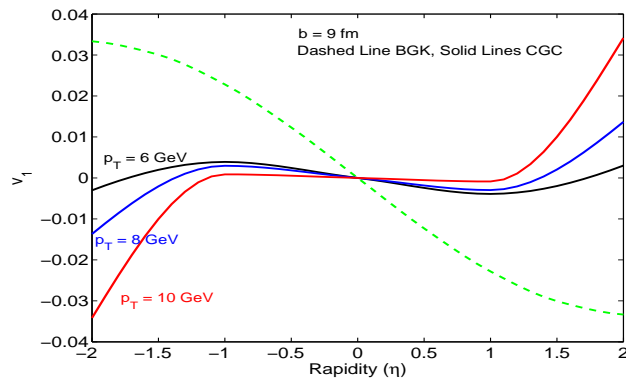


Figure 3. The directed flow v_1 as a function of η for different p_T at $b = 9$ fm. Both the CGC model and BGK model are given for comparison. This plot is from [1].

the system starts, and after that the system has gone through thermalization, a possible QGP phase, hadronic interactions and freeze out. A lot of early information can be easily washed out or completely lost due to various effects at later stages. Nevertheless, both theoretists and experimentalists begin to realize the importance of the initial condition, and starts to trace its footprints. Fig. 3 shows that for high p_T particles the v_1 (solid lines) from CGC flips sign at $\eta \simeq 1.2$, and becomes positive for higher values of rapidity. That means particles are flowing in the same direction as the projective spectator. In the conventional factorized jet production (dashed line), the high p_T v_1 is negative and in the same direction as the low p_T bulk directed flow. It would be interesting for experimentalists to test this novel prediction from CGC in the future. One can also exam the initial condition by studying the fluctuation of elliptic flow. Both STAR[8] and PHOBOS[9] collaboration has measured (see Fig.4) the v_2 fluctuation and compared it to the fluctuation from initial conditions assuming Glauber sources. The v_2 fluctuation

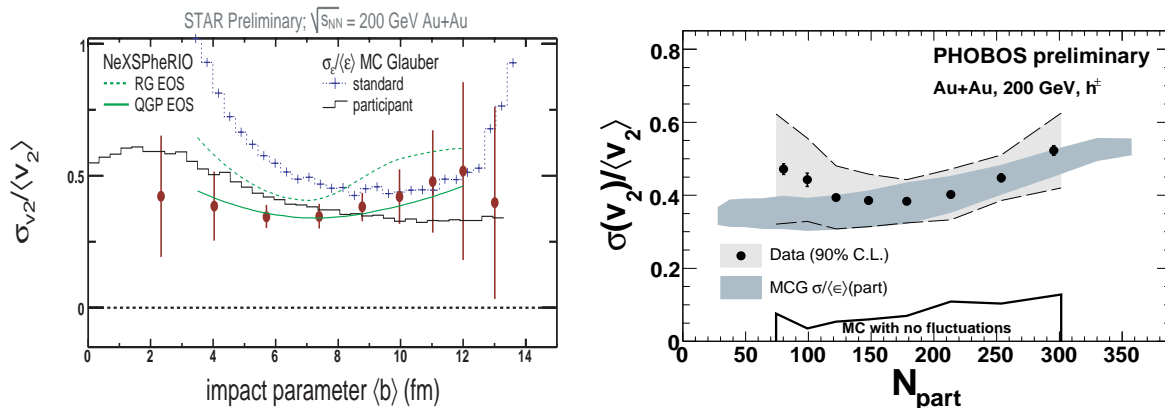


Figure 4. The r.m.s. width of the v_2 distribution (σ_{v_2}) scaled by the mean v_2 . Data are presented versus impact parameter (left by STAR) and number of participants (right by PHOBOS). In the left plot, together shown are eccentricity fluctuations $\sigma/\langle\epsilon\rangle$ calculated from the Monte-Carlo Glauber model with standard eccentricity (crosses) and participant eccentricity (step-line), the latter calculation is also done by PHENEX (dark contour in the right plot)

is found to be significant ($\sim 40\%$ relatively), and most of it can be explained by the fluctuation from the Glauber model as the initial condition. It means that, again, the conversion process from the initial spatial eccentricity to momentum anisotropy is so complete that little room is left for fluctuations of other dynamic processes.

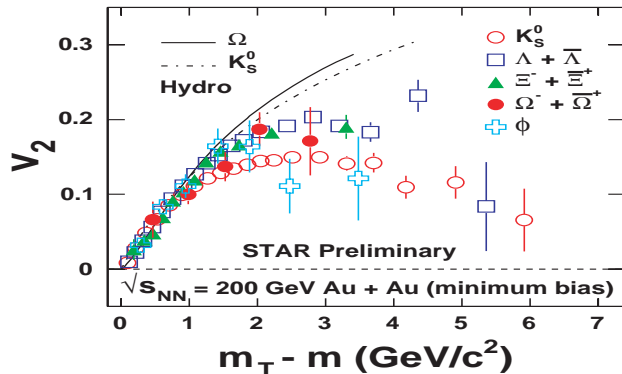


Figure 5. v_2 as a function of transverse kinetic energy for Multi-Strange baryons. Also shown is the Hydro calculation for Ω and k_s^0 . The data points are from [11].

3. Collectivity and thermalization

After the initial collision, particles begin to exchange momentum and the system begins to build up collectivity. Knowing when and how the collectivity is achieved is the first step towards understanding the dynamics in a hot and dense environment. This can be addressed by studying the v_2 of ϕ and Ω . Both of them are expected to have small hadronic cross section[10] thus are less affected by hadronic interactions. The other reason to choose ϕ for this purpose is because of its long lifetime – it decays outside of the fireball and is not formed by k^+k^- coalescence, thus it picks up little information from a later stage. Fig. 5 shows that, although ϕ and Ω tends to suffer much less rescatterings in the hadronic stage of the collision, their v_2 are found to be as high as other hadrons at a given p_T . Hence the collectivity must be developed fast at a pre-hadronic stage.

Building up collectivity does not necessarily mean that the system is thermalized. In order for the system to be thermalized, particles in the system have to “talk” to each other intensively so that the information like the initial spatial anisotropy can be passed on to all particles. This process depends on number of collisions encountered by each particle. It is expected that both v_2 and v_4 are proportional to the number of collisions per particle, and thus the ratio of v_4/v_2^2 decreases with it[12]. In Fig.6, this ratio is plotted against p_T and compared to theoretical calculations. The Hydro calculation done by Borghini and Jean-Yves[12] suggests that in ideal hydrodynamics, this ratio decreases as a function of p_T . Another version of Hydrodynamic calculation[13] shows a similar trend with smaller magnitude. The calculation from the AMPT[14] model shows a more or less flat shape. The data points are higher than theoretical calculations but the systematical errors are also large. It is desirable that in the future the uncertainty from both experiment measurement and theoretical calculation can be reduced, so that the degree of thermalization can be tested.

4. Scaling of soft physics

The number of collisions encountered by each particle on its way out not only plays an important role in thermalization, but also leads to a simple, but interesting scaling of soft physics. Fig. 7 shows that for different collision energies and over a wide range of

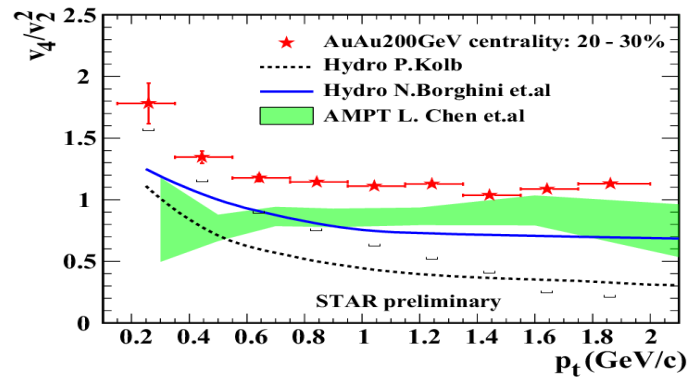


Figure 6. v_4/v_2^2 as a function of p_T . v_4 is measured by the three-particle cumulant method, and v_2 is measured by the four-particle cumulant method. Also shown are model calculations. This figure is from [15]

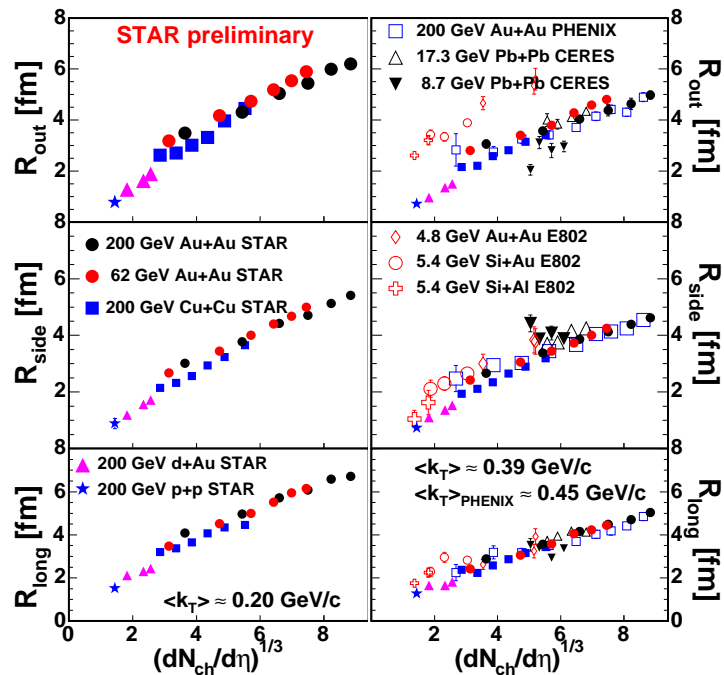


Figure 7. Femtoscentic radii dependence on the number of charged particles. Left panel: results from STAR experiment only for $\langle k_T \rangle \approx 0.20$ GeV/c; right panel: STAR results combined with data from PHENIX, CERES and E802 experiments, mean value of k_T is given on the plot. This plot is from [16].

collision systems, the HBT radii show a nice linearity if plotted against $dN/dy^{1/3}$, which is proportional to the source's length, and in turn relates to the number of interactions for a particle on its way out. R_{out} is an exception because it includes both space and time information thus the simple scaling with length is not expected. A similar $dN/dy^{1/3}$ scaling is also observed[17] in the strangeness yield relative to pp. Fig. 8 shows a good linearity if the relative yield of Ω and Ξ are plotted as a function of $dN/dy^{1/3}$. Also shown in the figure is the theoretical calculation of the enhancement with the correlation volume $V = (N_{part}/2)^\alpha V_o$, where $V_o = 4/3 \cdot \pi R^3$ and R is the radius of the proton. The curve which fits the shape of the data the best is for the case of $\alpha = 1/3$, which indicates that length plays an important role in strangeness production. Such linearity can be seen in flow measurements as well. In Fig. 9, the v_2 is scaled by the initial eccentricity and plotted as a function of particle's density $1/SdN/dY$, which is also proportional to the length of the system because dN/dY is proportional to the volume and S is the overlap area. Over a broad range of collision energies and system sizes, we observe a good linear relationship between v_2/ϵ and $1/SdN/dY$. This linear relation disappears if the same quantity plotted against N_{part} (Fig. 10), which is directly related to the volume.

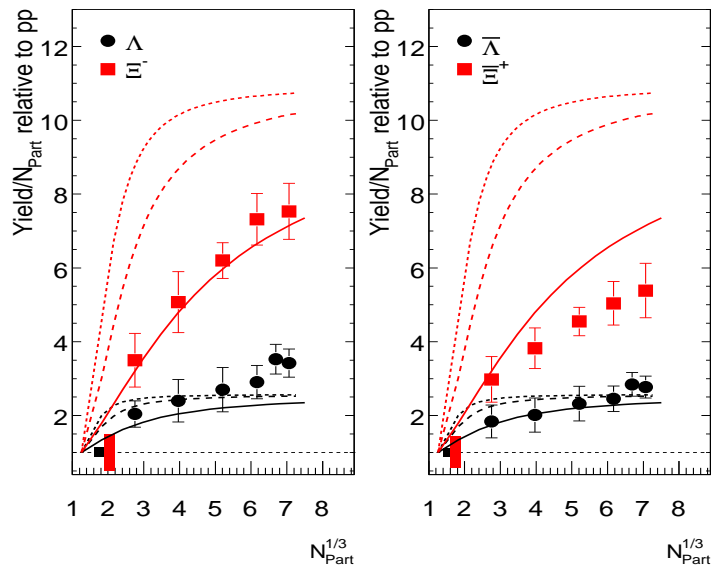


Figure 8. Strangeness enhancement as a function of p_T . Also shown are three theory curves which represent the evolution with collision participants (N_{part}) of the expected enhancement factors. The correlation volume for strangeness enhancement is calculated as $V = (N_{part}/2)^\alpha V_o$, where $V_o = 4/3 \cdot \pi R^3$ and R is the radius of the proton. The three curves correspond to values of α of 1 (short dashed line), 2/3 (long dashed line) and 1/2 (solid line) respectively. The figure is re-plotted based on Fig.2 in [17].

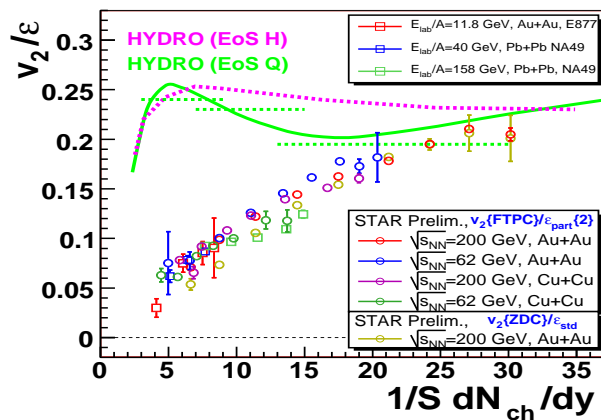


Figure 9. v_2/ϵ vs. $1/S dN/dy$ measured by the STAR Collaboration. Where S is the overlap area and dN/dy is the yield for charged particles at midrapidity. This plot is from [19].

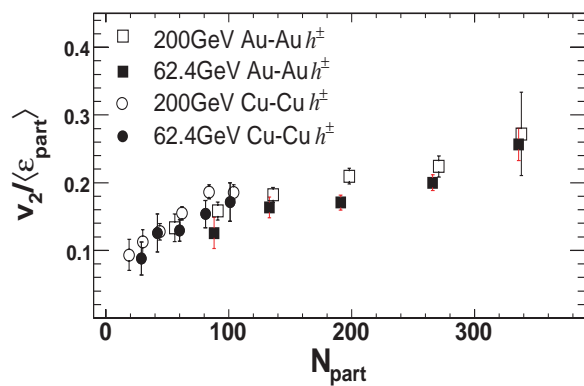


Figure 10. v_2 vs. N_{part} , for Cu+Cu and Au+Au collisions at $\sqrt{s_{NN}} = 62.4$ and 200 GeV. $1-\sigma$ statistical error bars are shown. This plot is from [20]

The simple linear scaling from three important sectors of soft physics (HBT, strangeness, flow) suggests that the number of collisions encountered by each particle plays an important role in soft physics. One may venture [18] to predict v_2 , HBT radii and the relative strangeness yield based on this simple scaling, without knowing anything about the collision (energy, system size etc.).

5. Directed flow

Directed flow (v_1) describes the “bounce-off” motion of particles away from midrapidity. As an important tool to probe the system at forward rapidity, it complements our understanding of the dynamics at midrapidity. Directed flow from different energies at SPS has been studied in [21], however its system size dependence has not been well explored. v_1 for Au+Au collisions at both $\sqrt{s_{NN}} = 62.4$ and 200 GeV have been measured[22], the Cu+Cu data that RHIC experiments collected in year 2005 at the same two energies gives us a good opportunity to study the system size dependence. The left plot in Fig. 11 presents v_1 as a function of pseudorapidity measured by the STAR Collaboration. Data from Cu+Cu collisions and Au+Au collisions at both energies

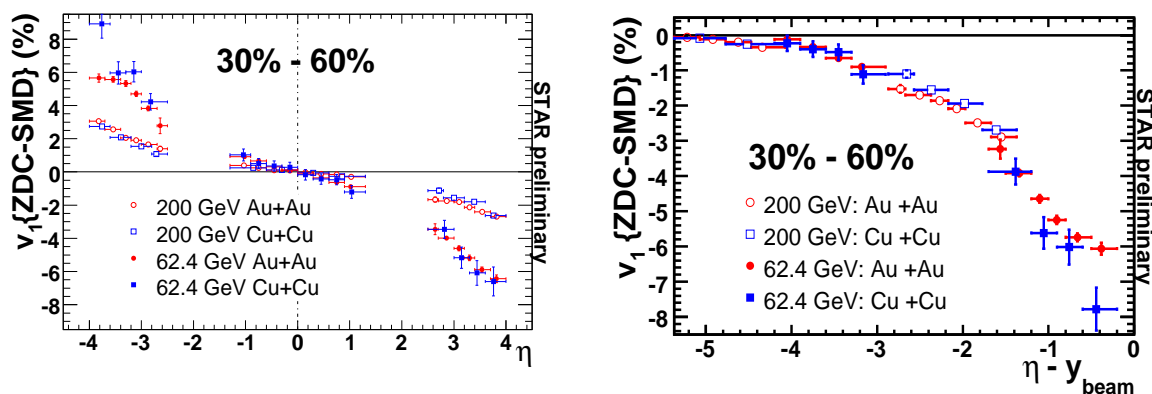


Figure 11. Left: Charged-hadron v_1 vs. η , for Au+Au and Cu+Cu collisions at $\sqrt{s_{NN}} = 62.4$ and 200 GeV. Right: The same data but plotted as a function of v_1 vs. $\eta - y_{beam}$. Both plots are from [23].

($\sqrt{s_{NN}} = 62.4$ and 200 GeV) are shown. The data points fall into two bands, one is for $\sqrt{s_{NN}} = 62.4$ GeV and the other one is for $\sqrt{s_{NN}} = 200$ GeV. From Au+Au collision to Cu+Cu collision the system size is reduced by 1/3, however the v_1 does not change. This is true even for the region near midrapidity, where v_2 for Cu+Cu collisions is considerably lower than that for Au+Au collisions [19]. Unlike v_2/ϵ which scales with system length, v_1 is found to be independent of system size. Instead, it scales with the incident energy. A possible explanation to the different scalings for v_2/ϵ and v_1 might come from the way in which they are developed: To produce v_2 , intensive momentum exchanges among particles are needed (and remember number of momentum exchanges is related to the length), while to produce v_1 , one in principle needs only different rapidity losses, which has a connection to the incident energy, for particles having different distances away from the central point of the collision.

One may also test the limiting fragmentation hypothesis[24], which has successfully described particle’s yield and flow at forward rapidity, with different system sizes. The right plot in Fig.11 re-plotted the same v_1 results as a function of $\eta - y_{beam}$. We can see that within three units from beam rapidity, most data points fall into a universal curve. This extends the validity of limiting fragmentation to different collision system

sizes. There are evidences[15] show that limiting fragmentation also works for higher harmonics like v_4 .

6. Summary

In summary, rich results from RHIC support a Hydrodynamic expansion of a thermalized fluid, in which the collectivity is achieved fast and at the very early time. Understanding the initial condition plays a key role in understanding what happens thereafter. Studying elliptic flow fluctuation, as well as directed flow for high p_T particles, may help us constraint the initial condition. A few key observables from soft physics are found scaling with system length, which is directly related to the average number of interactions for a particle on its way out. Directed flow is found to depend on the incident energy but not on the system size. Limiting fragmentation holds for different collision energies, systems and flow harmonics.

References

- [1] BRAHMS, PHENIX, PHOBOS, and STAR Collaboration, *Hunting the Quark Gluon Plasma: Results from the First 3 Years at RHIC* (Upton, NY: Brookhaven National Laboratory report No. BNL-73847-2005).
- [2] Ollitrault J-Y 1998 *Nucl. Phys. A* **638** 195c
Poskanzer A M and Voloshin S A 1998 *Phys. Rev. C* **58** 1671
- [3] BRAHMS, PHENIX, PHOBOS, and STAR Collaboration 2005 *Nucl. Phys. A* **757** Issues 1-2
- [4] Teaney D 2003 *Phys. Rev. C* **68** 034913
- [5] Adler C *et al* STAR Collaboration 2002 *Phys. Rev. C* **66** 034904
- [6] Glauber R J and Matthiae G 1970 *Nucl. Phys. B* **21** 135
Jacobs P and Cooper 2000 nucl-ex/0008015
- [7] Adil A *et al* 2006 *Phys. Rev. C* **74** 044905
Hirano T *et al* 2006 *Phys. Rev. B* **636** 299
- [8] Sorensen P for the STAR Collaboration 2007 Proceeding of this Quark Matter nucl-ex/0612021
- [9] Loizides C for the PHOBOS Collaboration 2007 Proceeding of this Quark Matter
- [10] Teaney D, Lauret J and Shuryak E V 2001 nucl-th/0110037
- [11] Lu Y private communication. Also shown by Bai Y for the STAR Collaboration 2007 Proceeding of this Quark Matter
- [12] Borghini N, and Ollitrault J.-Y. 2006 *Phys. Lett. B* **642** 227
- [13] Kolb P 2003 *Phys. Rev. C* **68** 031902
- [14] Chen L's AMPT calculation 2006 private communications
- [15] Bai Y for the STAR Collaboration 2007 Proceeding of this Quark Matter
- [16] Chajeccki Z. for the STAR Collaboration 2006 *Nucl. Phys. A* **774** 599
- [17] Lamont M for the STAR Collaboration 2006 *J. Physique G* **32** s105
- [18] Caines H 2006 *The Eur. Phys. J. C* 10.1140/epjc/s10052-006-0109-2
- [19] Voloshin S 2007 Proceeding of this Quark Matter nucl-ex/0701038
- [20] Alver B *et al* PHOBOS Collaboration 2006 nucl-ex/0610037
- [21] Alt C *et al* NA49 Collaboration 2003 *Phys. Rev. C* **68** 034903
- [22] Adams J *et al* STAR Collaboration 2004 *Phys. Rev. Lett.* **92** 062301
Adams J *et al* STAR Collaboration 2005 *Phys. Rev. C* 014904
- [23] Gang W for the STAR Collaboration 2007 Proceeding of this Quark Matter hep-ex/0701041
- [24] Benecke J, Chou T T, Yang C-N and Yen E 1969 *Phys. Rev.* **188** 2159